JOURNAL OF APPLIED POLYMER SCIENCE VOL. 19, PP. 959–972 (1975)

Thermal Degradation of Polymers. VII. Ablation Studies on a Series of Composite Specimens Containing Asbestos Fiber with Various High-Temperature Resin Binders

D. KERSHAW* and R. H. STILL, *Department of Polymer and Fibre Science, UMIST, Manchester, England,* and V. G. BASHFORD, *Polymer Technology Department, John Dalton Faculty of Technology, Manchester, England*

Synopsis

The use of a laboratory ablation test rig for the assessment of tubular asbestos-reinforced composites is described. Ablation resistance, char depth, smoke, and flash measurements have been made on a series of composites produced using asbestos fiber with a variety of commercially available high-temperature resin binders. The results have been compared with those obtained from a standard asbestos/phenolic composite and are discussed in terms of the properties of the composite and its components.

INTRODUCTION

In previous papers in this series,[1–6] thermal degradation studies on a series of substituted styrene polymers were reported. We now report the development and use of a laboratory ablation test rig for ablation studies on tubular specimens with facility for smoke and flash measurements.

A variety of tubular composite specimens containing asbestos fiber with different high-temperature resin binders have been studied to assess their potential for use as exhaust linings in rocket motors. In this context, the development of improved ablative insulation materials could permit highly desirable savings in rocket motor structure weight and volume. Low smoke evolution and flash characteristics (known as the signature problem) are also important design requirements for rocket motors as many devices are visually guided and the location of launch sites through "back tracking" tactical missiles is obviously undesirable.

The results obtained from the test rig have been correlated with the composite structures and the properties of the component parts.

EXPERIMENTAL

Apparatus

The apparatus used in these studies was described in detail previously[7,8] and is shown schematically in Figure 1. It consists essentially of three parts, an oxy-

* Present address: Kelvin Lenses Ltd., Denton Manchester, England.

© 1975 by John Wiley & Sons, Inc.

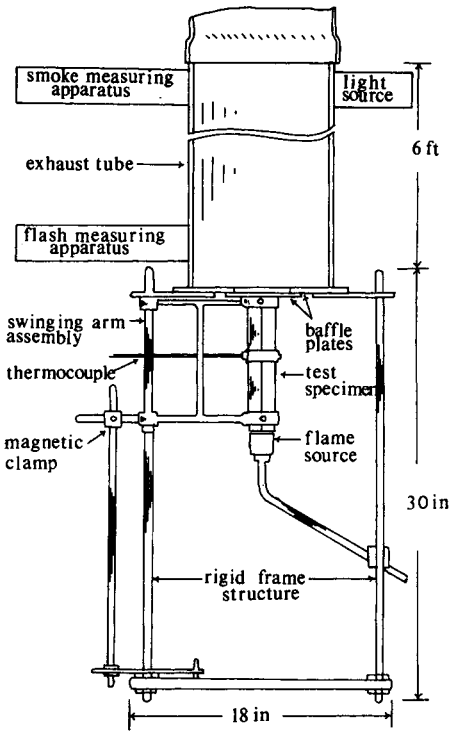

Fig. 1. Ablation test rig.

acetylene gas heating torch, a specimen clamp and swinging arm assembly which allows rapid precise location of the specimen in the preset test flame, and an exhaust tube containing the smoke- and flash-measuring equipment.

Tubular specimens (9 in. long × 1 in bore diameter × $^1/_4$ in. wall thickness) were used to simulate the rocket motor blast tube situation, split longitudinally to overcome manufacturing difficulties. A sheathed Chromel–Alumel thermocouple $^1/_{16}$ in. in diameter was located centrally in one half of the specimen with the hot junction 0.1 in. from the inside surface. This yielded a suitable time-temperature profile whilst limiting the duration of the test to retain a layer of virgin material on the specimen to permit the measurement of char depths.

Quantitative measurements of smoke evolution were made by monitoring the obscuration of a standardized light source by means of a cadmium sulfide photoelectric cell. These units were located at a sufficient distance above the flame source to ensure that the outputs recorded were not influenced by thermal or illumination effects from the flame during test.

An assessment of the flash characteristics of the material was obtained using a selenium self-generating photoelectric cell to monitor the light intensity of the test flame emerging from the specimen.

A neutral oxy-acetylene flame (oxygen:acetylene 1:1) was used to produce the highest temperature nonoxidative flame capable of allowing the specimen to be swung into position. Maximum flame intensity was achieved using an oxygen pressure of 30 lb/in^2., flow rate 60 ft^3/hr in conjunction with acetylene at 18 lb/in.^{2}, and the same flow rate.

TABLE I
Resin Binder Systems

Resin no.	System	Source
1	Phenol-formaldehyde resin CS303	Carborundum Co. Ltd.
2	Phenol-formaldehyde resin CS311	Carborundum Co. Ltd.
3	Xylok 210	Albright and Wilson Ltd.
4	Polyphenylene 1711	Monsanto Ltd.
5	Epoxy–Novalak, 154/NMA/BDMA	Shell Chemicals Ltd.
6	Cycloepoxy, ERLA 4617/DDM	Union Carbide Ltd.
7	Polyimide P13N	TRW Systems Inc.
8	Polyimide QX13	ICI Ltd.
9	Silicone MS2106	Dow Corning Ltd.
10	Polyester 17449	Bakelite Ltd.

Ablation Test Operating Procedure

The specimen halves, after drilling to accept the thermocouple and weighing, were assembled together in the swinging arm assembly (Fig. 1) and aligned relative to the torch tip and the exhaust tube. The specimen was then swung away to permit ignition and stabilization of the flame source. To commence the test, the specimen was swung rapidly into position and automatically locked. During the 3-min duration of the test thermocouple output, smoke and flash were continuously recorded. At the end of 3 min, the locking mechanism was released allowing the specimen to swing away from the flame into a nitrogen stream to minimize post test oxidative degradation during cooling.

Materials

Various commercially available resin systems were chosen, on the basis of their reported temperature stability, and used to produce composite specimens incorporating asbestos fiber as the discrete reinforcement phase. A standard flock form of chrysotile asbestos fiber, FR91, supplied by Turner Brothers Asbestos Ltd., was used.

The resin systems investigated are shown in Table I. Durestos RA51 ex Turner Brothers Asbestos was used as a control material, supplied as a preblended molding material containing a nominal 59% by weight of FR91 asbestos flock, in a phenol–formaldehyde novolak resin binder.

Specimen Preparation

The tests specimens were manufactured in two halves, molded simultaneously in a twin-impression, compression-molding tool. This allowed readily loading of the high-bulk factor fiber-reinforced molding compound and produced randomly oriented composites, without the molding problems normally associated with tubular components. The control material was preformed to reduce to its bulk factor and molded at 150°C for 30 min. For materials 1–10 and asbestos fiber FR91, mixing formulations were designed to produce moldings containing a nominal 44% fiber by volume. The methods adopted to produce the mixed fiber/resin compounds varied with the particular materials under consideration. All molding materials were blended initially in a laboratory size Z blade mixer. The fiber was loaded first and premixed to open out the structure and break down

TABLE II
Specimen Molding and Curing Conditions

Resin component	Mold preheat temp., °C	Dwell time, min	Cure cycle time/temp., min/°C	Postcure schedule
Phenolic CS303	160	1	30/160	nil
Phenolic CS303	160	1	30/160	6 hr/200°C
Phenolic CS311	160	1	30/160	nil
Phenolic CS311	160	1	30/160	6 hr/200°C
Xylok 210	175	0.5	30/175	6 hr/175°C
Polyphenylene 1711	310	5	240/310[a]	4 hr/175°–240°C 13 hr/250°C 24 hr/275°C 24 hr/300°C 24 hr/325°C
Epoxy-Novolak 154/NMA/DMA	120	1	30/120[b] 150/150	16 hr/200°C
Epoxy ERLA 4617/DDM	160	1	60/160	16 hr/160°C
Polyimide P13N	290	0.5	60/290[b]	nil
Polyimide QX13	320	2	30/320	5 hr/150°–300°C 16 hr/300°C 2 hr/300°–320°C
Silicone resin MS2106	175	1	45/175[a]	nil
Polyester 17449	100	0.5	2/100	16 hr/160°C

[a] Cooled to 100°C under pressure.
[b] Cooled to 30°C under pressure.

agglomerations. The resin was then added and the mixing continued for a further 10–15 min.

Phenolic resins were added in fine powder form as supplied. Other resins were added to the fibers in solution form to ensure complete impregnation and wetting of the fibers during the mixing stage. Following drying and precuring cycles, where necessary, the molding materials were finally ground by passing once through a Christy and Norris grinding machine.

The required weight of the fiber/resin blend was preformed to reduce the very high bulk factor, and the specimens were molded and press cured according to the schedules given in Table II. Postcuring was carried out in an air circulating oven or furnace, and heating and cooling rates of 2°C/min (nominal) were employed.

Measurements Performed on Tubular Specimens

Prior to Test. The specimens were molded 10 in. long to provide a 1-in. off-cut sample for fiber content determination and other tests. After trimming to length, the specific gravity of each molding was determined and wall thickness measurements were made at 1-in. intervals along the center line. Fiber contents were determined by ignition in a furnace at 900°C in air to constant weight.

Post Test Measurements. Weight loss determinations were carried out on all samples after testing on the ablation rig. After weighing, the char structure of each specimen was sealed using a cold-curing liquid epoxy resin system (CIBA MY753 + HY956 cured 16 hr at room temperature). After sectioning along the center line and polishing, char depths were measured at 1-in. intervals (coincident

TABLE III
Weight Loss Fiber Content and Specific Gravity Measurements

Material[a]	Fiber content, %	sp. gr.	Weight loss, %
RA51 control	58.4	1.74	28.0
A/Phenolic CS303	63.2	1.80	23.7
A/Phenolic CS303 (postcured)	63.7	1.76	23.4
A/Phenolic CS311	61.8	1.79	24.6
A/Phenolic CS311 (postcured)	63.6	1.77	23.8
A/Polyimide P13N	63.9	1.79	26.3
A/Polyimide QX13	64.4	1.81	27.4
A/Polyphenylene 1711	63.0	1.55	25.4
A/Xylok 210	60.1	1.71	23.7
A/Epoxy 154/NMA/BDMA	61.3	1.81	28.0
A/Epoxy 4617/DDM	63.8	1.81	32.4
A/Polyester 17449	63.5	1.81	31.6
A/Silicone MS2106	62.4	1.71	short firing

[a] A = Asbestos.

with the previous wall thickness measurements) using a traveling microscope. Visual assessment of char structure was also carried out.

RESULTS AND DISCUSSION

Table III shows the weight loss results obtained from the ablation test rig. Considering the severity of the test environment, all the materials show remarkable resistance, and only small differences in the weight losses observed are apparent. Two main factors contribute to this latter effect. Firstly, the specimens are not fully charred; the test was designed to leave a layer of virgin material approximately $^1/_{16}$ in. thick to facilitate char depth measurements. Secondly, the resin component undergoing the char reactions represents only some 40% by weight of the total composite. The weight loss has, however, been quoted as a percentage of the total composite as, in addition to the resin char reactions, erosion effects can take place which affect the total composite.

Table III shows that all the composite specimens produced have slightly higher fiber contents than the Durestos RA51 specimen. This arises as a result of the method of manufacture (Durestos RA51 control was supplied as a preblend) and because the specific gravity of asbestos can vary from 2.4 to 2.6.

If the Durestos RA51 result is factored to bring the initial fiber content to 63%, an average weight loss of 26% is obtained. From this it can be seen that the newer phenolic resins CS303 and CS311 together with Xylok 210 show slightly improved behavior, the polyimides and polyphenylene show similar characteristics and the epoxy and polyester materials show inferior performance in weight loss terms.

No weight loss result can be quoted for the silicone/asbestos specimen as it burnt out completely after 150 sec.

Char Thickness Results

These are shown in Table IV, position 1 indicating the flame entry end of the specimen. It was shown previously[7] that with the Durestos RA51 specimens, reproducibility is good considering the severity of the test conditions. All such

TABLE IV

Char Thickness Measurements. Sectioned Test Specimen

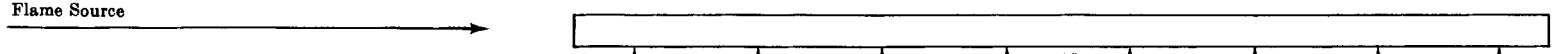

Material	Position	Measurement Position[a] 1	2	3	4	5	6	7	8
		1	2	3	4	5	6	7	8
Durestos RA51 control	Initial thickness	0.276	0.280	0.283	0.284	0.283	0.283	0.282	0.281
	Final thickness	0.265	0.284	0.308	0.343	0.327	0.354	0.354	0.354
	Thickness change	−0.011	+0.004	+0.025	+0.059	+0.044	+0.071	+0.072	+0.073
	Virgin material	0.043	0.051	0.075	0.102	0.106	0.106	0.108	0.103
	Char thickness	0.222	0.233	0.283	0.241	0.221	0.248	0.246	0.251
	Comments	fairly dense char showing some cracking and a smooth inside surface							
Asbestos/phenolic CS303	Initial thickness	0.266	0.266	0.266	0.265	0.263	0.263	0.261	0.259
	Final thickness	0.300	0.276	0.296	0.320	0.324	0.319	0.312	0.319
	Thickness change	+0.034	+0.010	+0.030	+0.075	+0.061	+0.056	+0.049	+0.060
	Virgin material	0.051	0.036	0.028	0.047	0.075	0.063	0.083	0.189
	Char thickness	0.249	0.240	0.268	0.273	0.249	0.256	0.229	0.130
	Comments	dense char, showing a good deal of cracking and a smooth inside surface							
Asbestos/phenolic CS303 postcured	Initial thickness	0.271	0.273	0.284	0.279	0.268	0.270	0.268	0.266
	Final thickness	0.256	0.236	0.260	0.268	0.256	0.282	0.286	0.296
	Thickness change	−0.015	−0.037	−0.024	−0.011	−0.012	+0.012	+0.018	+0.030
	Virgin material	0.102	0.063	0.032	0.032	0.055	0.063	0.128	0.130
	Char thickness	0.154	0.173	0.228	0.236	0.201	0.219	0.158	0.166
	Comments	dense char, showing slight cracking and a smooth inside surface							
Asbestos/phenolic CS311	Initial thickness	0.282	0.282	0.280	0.278	0.275	0.274	0.272	0.270
	Final thickness	0.304	0.282	0.286	0.323	0.315	0.331	0.335	0.342
	Thickness change	+0.022	0	+0.006	+0.045	+0.040	+0.057	+0.063	+0.072
	Virgin material	0.073	0.043	0.051	0.079	0.099	0.114	0.154	0.154
	Char thickness	0.231	0.239	0.235	0.246	0.216	0.217	0.181	0.188
	Comments	dense char, showing some cracking and a smooth inside surface							

Asbestos/phenolic CS311 (postcured)	Initial thickness	0.272	0.275	0.275	0.275	0.275	0.275	0.275	0.273
	Final thickness	0.248	0.232	0.272	0.280	0.280	0.280	0.304	0.288
	Thickness change	−0.024	−0.043	−0.003	+0.015	+0.005	+0.005	+0.029	+0.015
	Virgin material	0.043	0.039	0.055	0.043	0.055	0.087	0.110	0.177
	Char thickness	0.205	0.193	0.217	0.237	0.225	0.193	0.194	0.111
	Comments	dense char, showing slight cracking and a smooth inside surface							
Asbestos/polyimide P13N	Initial thickness	0.296	0.297	0.296	0.294	0.293	0.291	0.290	0.287
	Final thickness	0.288	0.298	0.304	0.296	0.296	0.294	0.300	0.296
	Thickness change	−0.008	+0.001	+0.008	+0.002	+0.003	+0.003	+0.010	+0.009
	Virgin material	0.110	0.102	0.043	0.086	0.094	0.099	0.087	0.158
	Char thickness	0.178	0.196	0.261	0.210	0.202	0.195	0.213	0.138
	Comments	dense char, very little cracking; yellow/orange color; hard, white foam exudate							
Asbestos/polyimide QX13	Initial thickness	0.257	0.258	0.258	0.258	0.259	0.258	0.258	0.259
	Final thickness	0.276	0.256	0.256	0.260	0.233	0.240	0.260	0.272
	Thickness change	+0.019	−0.002	−0.002	+0.002	−0.026	−0.018	+0.002	+0.013
	Virgin material	0.150	0.055	0.040	0.028	0	0	0.059	0.106
	Char thickness	0.126	0.201	0.216	0.232	0.233	0.240	0.201	0.166
	Comments	dense char; yellow-orange color; large amount of hard white foam exudate							
Asbestos/polyphenylene 1711	Initial thickness	0.284	0.288	0.288	0.289	0.287	0.287	0.287	0.286
	Final thickness	0.264	0.244	0.268	0.292	0.280	0.323	0.330	0.320
	Thickness change	−0.020	−0.044	−0.020	+0.003	−0.007	+0.036	+0.043	+0.034
	Virgin material	0.024	0.071	0.043	0.039	0.036	0.106	0.134	0.165
	Char thickness	0.240	0.173	0.215	0.253	0.244	0.217	0.196	0.155
	Comments	dense char, showing slight cracking and an uneven inside surface							
Asbestos/Xylok 210	Initial thickness	0.268	0.269	0.271	0.270	0.270	0.267	0.264	0.263
	Final thickness	0.272	0.236	0.284	0.256	0.254	0.264	0.268	0.264
	Thickness change	+0.004	−0.033	+0.013	−0.014	−0.016	−0.003	+0.004	+0.001
	Virgin material	0.055	0.024	0.035	0.020	0.026	0.031	0.099	0.190
	Char thickness	0.217	0.202	0.249	0.236	0.228	0.233	0.169	0.074
	Comments	inside surface very rough showing a "fibrous" type of char growth							

(*continued*)

TABLE IV (*continued*)

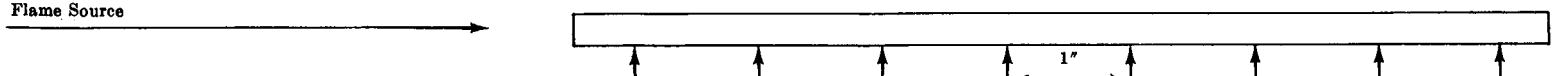

Material	Position	Measurement Position[a] 1	2	3	4	5	6	7	8
		1	2	3	4	5	6	7	8
Asbestos/epoxy 154/NMA/BDMA	Initial thickness	0.263	0.262	0.262	0.260	0.261	0.261	0.261	0.260
	Final thickness	0.236	0.268	0.300	0.280	0.256	0.285	0.288	0.256
	Thickness change	−0.027	+0.006	+0.038	+0.018	−0.005	+0.024	+0.027	−0.004
	Virgin material	0.075	0.083	0.067	0.102	0.110	0.108	0.125	0.110
	Char thickness	0.161	0.185	0.233	0.178	0.146	0.177	0.163	0.146
	Comments	slightly porous char, inside surface rough							
Asbestos/epoxy 4617/DDM	Initial thickness	0.261	0.261	0.265	0.267	0.268	0.267	0.265	0.262
	Final thickness	0.240	0.256	0.260	0.280	0.300	0.284	0.288	0.296
	Thickness change	−0.021	−0.005	−0.005	+0.013	+0.032	+0.017	+0.023	+0.034
	Virgin material	0.047	0.047	0.043	0.059	0.051	0.071	0.154	0.162
	Char thickness	0.193	0.209	0.217	0.221	0.249	0.213	0.134	0.134
	Comments	very porous char; char/virgin interface difficult to determine accurately							
Asbestos/polyester 17449	Initial thickness	0.256	0.257	0.256	0.255	0.256	0.257	0.256	0.257
	Final thickness	0.300	0.240	0.205	0.220	0.288	0.284	0.280	0.280
	Thickness change	−0.044	−0.037	−0.051	−0.035	+0.032	+0.027	+0.024	+0.023
	Virgin material	0.067	0.075	0.071	0.083	0.091	0.126	0.106	0.118
	Char thickness	0.233	0.165	0.134	0.137	0.197	0.158	0.174	0.162
	Comments	very porous char; char/virgin interface difficult to determine accurately							
Asbestos/silicone MS2106		no measurements taken; short firing; very poor char structure with a rough inside surface							

[a] All measurements in inches.

samples showed a dense char structure with the char–virgin material interface very apparent. The thickness measurement variations 1–8 are attributable to varying flame conditions along the tube, positions 1 and 2 coinciding with the hottest part of the flame. Little or no material appears to have been removed by erosion.

The asbestos/phenolic CS303 and CS311 specimens show similar behavior to the Durestos RA51 control in the non-postcured state. Differences are found with the two postcured samples in that, while the virgin material thicknesses remain comparable, both postcured samples show less resistance to erosion in that final specimen thicknesses are reduced. This may be caused by the "as molded" materials being tougher and more resistant to erosion, or more probably arises as a result of additional cure reaction products volatilizing and adding to the overall ablative cooling effect.

Effects similar to those seen with the postcured phenolic specimens are apparent with the polyimide and polyphenylene materials where the final thickness results are again less than those obtained with the "as molded" phenolic materials. The polyimide materials would appear, from visual examination, to have experienced higher surface temperatures in that a hard, white foam exudate, probably silicaceous material from the asbestos, was apparent around positions 1, 2, and 3.

The asbestos/Xylok 210 specimen exhibited a unique char structure, the inside surface being very rough with the char having "grown" to produce a quasi-fibrous structure. The asbestos/epoxy and asbestos/polyester specimens showed porous char structures which account for the higher weight loss results shown in Table II. In addition, the char–virgin material interface was less clearly defined. In the higher erosion environment of a rocket motor, such porous char structures would be easily removed.

Specimen Time–Temperature Profiles

Previous work[7] has shown the reproducibility of the time–temperature profiles for the Durestos RA51 composite control specimens. It can be seen from Figures 2, 3, and 4 that all the specimen time–temperature graphs show a similar profile with a slow rate of temperature increase over the first 60 sec. The rate of temperature rise then becomes more rapid as the char–virgin material interface moves back into the specimen and through the thermocouple position and finally levels out in the 700°–900°C region as pseudo-steady-state ablation is achieved.

Figure 2 compares the behavior of the asbestos–phenolic resin composites. Differences are observed in the performance of the "as molded" and postcured samples, with the profiles for the postcured materials reading 300°C some 20 sec earlier than the "as molded" materials. This effect can be attributed to the "as molded" materials undergoing further cure reactions liberating low molecular weight reaction products which contribute to the overall ablation cooling effect. Thus, improved ablation performance can be achieved without compromising the upper region of the time–temperature curve and with a minimal weight penalty (see Table III weight loss results).

Figure 3 shows the behavior of the newer high-temperature systems investigated. The polyimide QX13 and the polyphenylene 1711 specimens both show plateau effects in the 100°–150°C region, again suggesting that further cure reactions are occurring accompanied by the liberation of low molecular weight

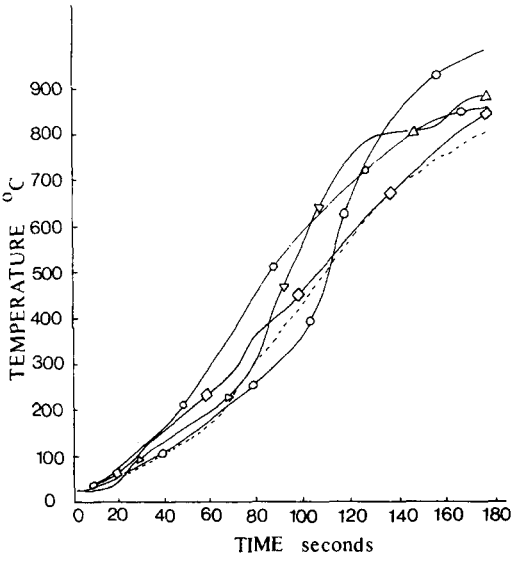

Fig. 2. Time–temperature profiles for phenolic resin specimens: (———) Durestos RA51 control; (—△—) A*/phenolic resin CS303; (—○—) A/phenolic resin CS303, postcured; (—○—) A/phenolic resin CS311; (—□—) A/phenolic resin CS311, postcured. *A = Asbestos.

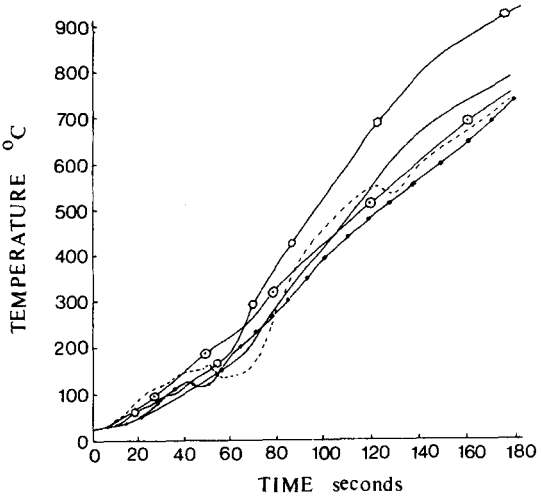

Fig. 3. Time–temperature profiles for new high-temperature resin systems: (———) Durestos RA51 control; (—○—) A*/polyimide P13N; (●—●—●) A/polyimide QX13; (- - - -) A/polyphenylene 1711; (—○—) A/Xylok 210. *A = Asbestos.

volatile products. That the polyimide P13N profile shows a change in slope rather than a plateau may be explained by it being a more rapid curing system which does not require a postcure schedule. The polyphenylene 1711 specimen shows a second plateau effect in the 500°C region, which would appear to be linked with some endothermic reaction occurring in that region. The Xylok 210 specimen again shows a typical profile for a postcured material.

Figure 4 compares the behavior of the more traditional high-temperature resin systems. The epoxy materials show significantly reduced temperature increases but not without cost in that more material has been sacrificed (see Table III).

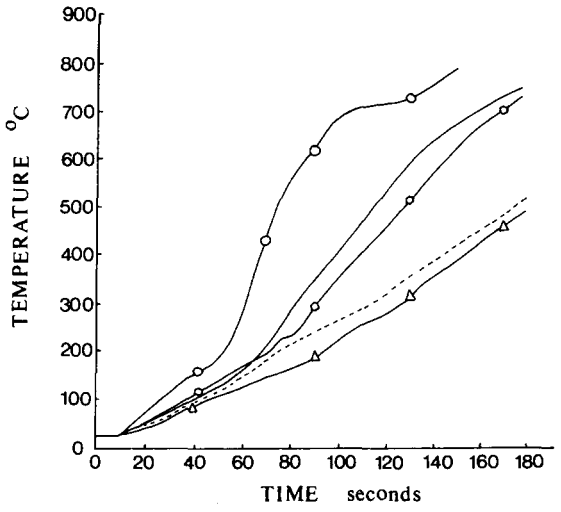

Fig. 4. Time-temperature profiles for traditional high-temperature resin systems: (———) Durestos RA51 control; (– – –) A*/epoxy 154/NMA/BDMA; (—△—) A/epoxy 4617/DDM; (—○—) A/polyester 17449; (—○—) A/silicone MS2106. *A = Asbestos.

The polyester material shows a similar profile to the control specimen but again loses significantly more weight (Table III).

The silicone composite specimen showed very poor ablative performance with a rapid initial temperature rise, and it failed to survive the full test period.

Smoke Obscuration Results

Figures 5, 6, and 7 show the smoke obscuration traces obtained with the various composite specimens. Reproducibility with the Durestos RA51 speci-

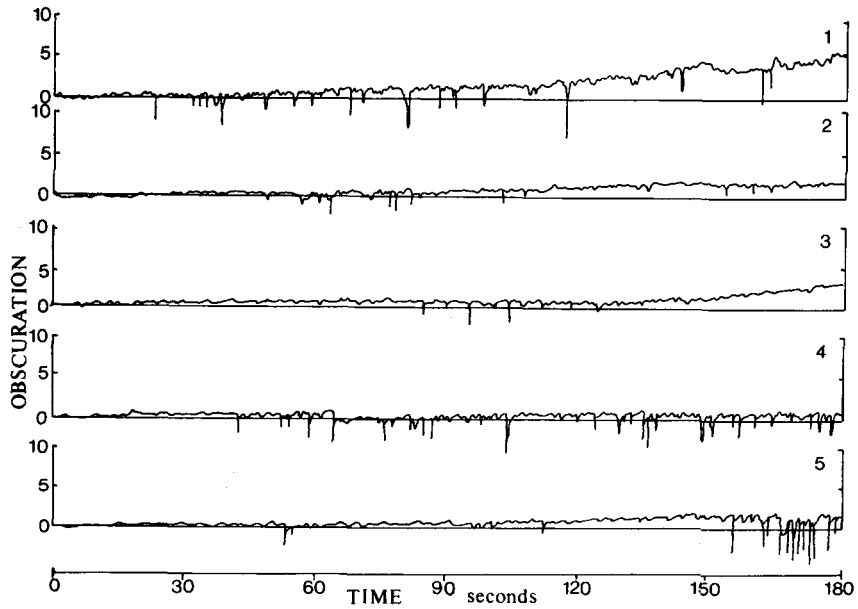

Fig. 5. Smoke obscuration traces: (1) Durestos RA51 control; (2) A*/phenolic CS303; (3) A/phenolic CS303, postcured; (4) A/phenolic CS311; (5) A/phenolic CS311, postcured. *A = Asbestos.

mens was previously shown to be good,[8] and the trace shown is typical with ~2% obscuration after 90 sec rising to ~5% obscuration after 180 sec. The reproducibility of the four specimens is excellent, and there are no apparent differences caused by postcuring the samples.

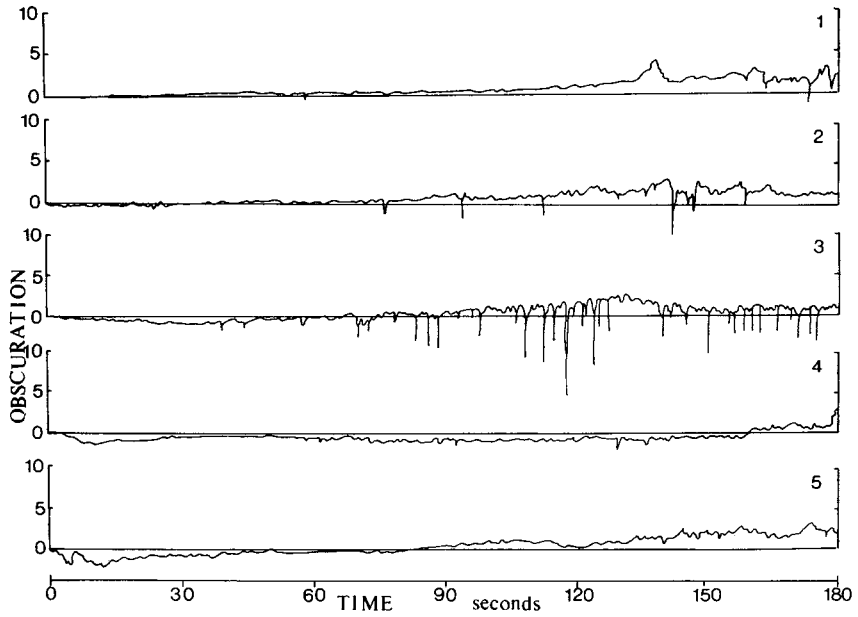

Fig. 6. Smoke obscuration traces: (1) A*/polyimide P13N; (2) A/polyimide QX13; (3) A/polyphenylene 1711; (4) A/Xylok 210; (5) A/epoxy 154/NMA/BDMA. *A = Asbestos.

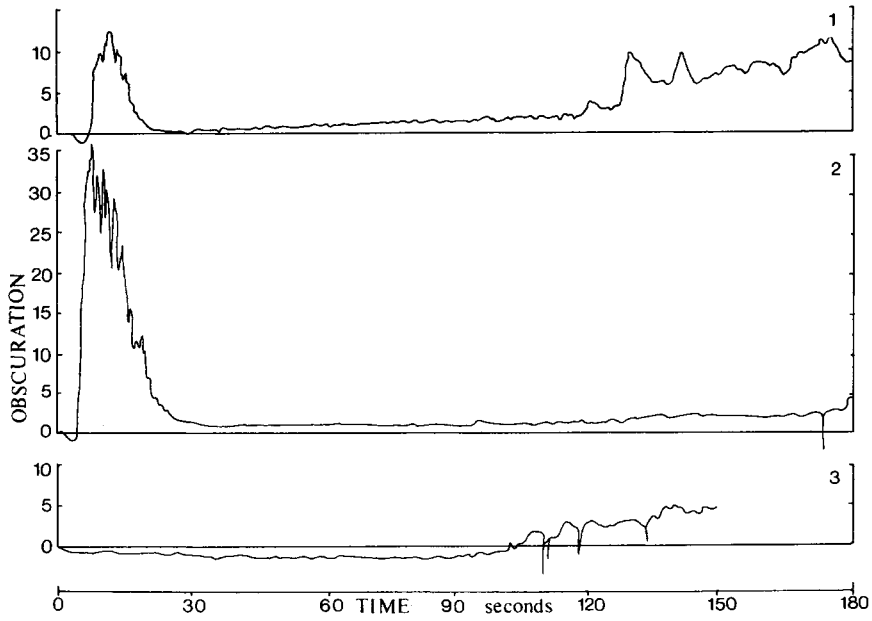

Fig. 7. Smoke obscuration traces: (1) A*/epoxy 4617/DDM; (2) A/polyester 17449; (3) A/silicone MS2106. *A = Asbestos.

Smoke evolution by the polyimide and polyphenylene resin composites is again low, particularly over the first 120 sec. The peculiar "flashing" behavior of the polyphenylene material may be attributed to glowing particles being removed from the specimen borne out by a more uneven final inside surface. The Xylok 210 and to a lesser extent the Epoxy 154/NMA/BDMA specimen show somewhat anomalous behavior in that the smoke traces fall below the zero axis.

This arises as a result of the specimens exhibiting a "char growth" effect which produces a very rough inside surface and reduces the bore diameter of the specimen causing elongation of the test flame which subsequently affects the monitoring equipment.

The asbestos/epoxy 4617 and the asbestos/polyester specimen both show increased smoke evolution, particularly in the early states as the resin is removed. This is followed by lower smoke emission due to the protective action of the asbestos fiber.

The silicone specimen initially shows a trace dipping below the zero axis, but in this case erosion effects lead to smoke emission (as shown by the test) after 120 sec (note early failure).

Flash Measurement Results

The flash measurement results obtained as a direct reading in volts from the self-generating selenium photoelectric cell are shown in Figure 8. Reproducibility of the Durestos RA51 results was again good as shown previously,[8] and the control trace shown is typical. By comparison, the newer phenolic materials show significant improvement, the output traces taking much longer to reach the same final value of 0.5 volts irrespective of the cure/postcure schedule.

The two polyimide materials show different behavior characteristics, the asbestos/QX13 specimen behaving similarly to the CS303 and CS311 phenolic

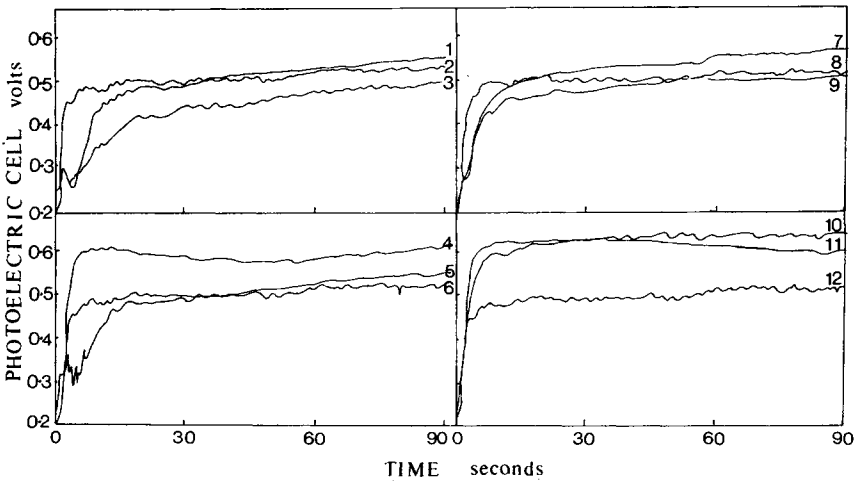

Fig. 8. Flash measurements: (1) A*/phenolic resin CS303, postcured; (2) Durestos RA51 control; (3) A/phenolic resin CS303; (4) A/polyimide P13N; (5) A/polyimide QX13; (6) Durestos RA51 control; (7) A/phenolic resin CS311, postcured; (8) Durestos RA51; (9) A/phenolic resin CS311; (10) A/silicone MS2106; (11) A/polyphenylene 1711; (12) Durestos RA51 control. *A = Asbestos.

materials, while asbestos/P13N behaves in a manner more comparable with the Durestos RA51 control but with a slightly higher output level of 0.6 volts.

The remainder of the resin specimens all show inferior flash behavior to the Durestos RA51 specimen, rapidly reaching output voltages of 0.6 volts and above as shown for asbestos/polyphenylene 1711 and asbestos/silicone MS2106 samples (Fig. 8).

CONCLUSIONS

Considering the ablative insulation properties only, remarkably few differences have been found in the behavior of the different classes of composites studied. Phenolic resins appear to offer the best combination of properties, particularly when their ease of handling and molding is taken into account. The newer phenolic resins investigated (CS303 and CS311) show similar ablative performance to the control material but with markedly reduced smoke obscuration. Thus, these materials could be used to advantage in rocket motors to improve the "signature" characteristics.

The authors thank Imperial Metal Industries, Summerfield Research Station for a Research Studentship (to D.K.) and for a grant. The authors also thank Mr. M. J. Chase for useful discussions.

References

1. R. H. Still and C. J. Keattch, *J. Appl. Polym. Sci.*, **10**, 193 (1966).
2. R. H. Still and P. B. Jones, *J. Appl. Polym. Sci.*, **13**, 401 (1969).
3. R. H. Still and P. B. Jones, *J. Appl. Polym. Sci.*, **13**, 2033 (1969).
4. R. H. Still and P. B. Jones, *J. Appl. Polym. Sci.*, **13**, 1555 (1969).
5. R. H. Still, M. B. Evans, and A. Whitehead, *J. Appl. Polym. Sci.*, **16**, 3207 (1972).
6. R. H. Still and A. Whitehead, *J. Appl. Polym. Sci.*, **16**, 3223 (1972).
7. D. Kershaw, R. H. Still, V. G. Bashford, and S. J. Hurst, *Chem. Ind.*, 95 (1973).
8. D. Kershaw, M.Sc. Thesis, Victoria University of Manchester, England, 1972.

Received July 25, 1974
Revised September 23, 1974